Resource

Conservation of mRNA and Protein Expression during Development of *C. elegans*

Dominic Grün,[1,3] Marieluise Kirchner,[2,3] Nadine Thierfelder,[1,3] Marlon Stoeckius,[1] Matthias Selbach,[2] and Nikolaus Rajewsky[1,*]

[1]Systems Biology of Gene Regulatory Elements, Max Delbrück Center Berlin, Robert-Rössle-Strasse 10, 13125 Berlin, Germany
[2]Cell Signalling and Mass Spectrometry, Max Delbrück Center Berlin, Robert-Rössle-Strasse 10, 13125 Berlin, Germany
[3]These authors contributed equally to this work
*Correspondence: rajewsky@mdc-berlin.de

SUMMARY

Spatiotemporal control of gene expression is crucial for development and subject to evolutionary changes. Although proteins are the final product of most genes, the developmental proteome of an animal has not yet been comprehensively defined, and the correlation between mRNA and protein abundance during development is largely unknown. Here, we globally measured and compared protein and mRNA expression changes during the life cycle of the nematodes *C. elegans* and *C. briggsae*, separated by ~30 million years of evolution. We observed that developmental mRNA and protein changes were highly conserved to a surprisingly similar degree but were poorly correlated within a species, suggesting important and widespread posttranscriptional regulation. Posttranscriptional control was particularly well conserved if mRNA fold changes were buffered on the protein level, indicating a predominant repressive function. Finally, among divergently expressed genes, we identified insulin signaling, a pathway involved in lifespan determination, as a putative target of adaptive evolution.

INTRODUCTION

Changes in gene expression are the basis of metazoan development. A new life starts with a totipotent zygote and requires many rounds of cell divisions and differentiation events to develop into a complex adult organism with a large diversity of tissues and cell types. Orchestrated differentiation of multiple cells within the developing animal is frequently driven by spatial or temporal changes in gene expression. Well-studied examples are spatial gene expression gradients that control the patterning of the *Drosophila* embryo (St Johnston and Nüsslein-Volhard, 1992) or temporal expression gradients of heterochronic genes in nematodes regulating the progression of larval development (Ruvkun and Giusto, 1989; Johnstone and Barry, 1996; Moss, 2007). Developmental gene expression is highly conserved, and alterations in gene expression levels are strong drivers of evolution

(Carroll, 2008; Haerty et al., 2008; Domazet-Lošo and Tautz, 2010; Kalinka et al., 2010). Comparing gene expression patterns across different species therefore provides insights into fundamental principles of development and evolution (Domazet-Lošo and Tautz, 2010; Kalinka et al., 2010; Levin et al., 2012). Notably, most of these conclusions were drawn from studies only interrogating transcript expression levels. However, gene expression is controlled at all molecular layers from genomic DNA to proteins, and changes in mRNA abundance are often a poor proxy for protein level changes (de Sousa Abreu et al., 2009; Schwanhäusser et al., 2011). Comprehensive simultaneous quantification of transcript and protein levels over the lifecycle of an organism would provide a highly informative data set describing developmental gene expression control. In particular, these data permit a quantification of the impact of posttranscriptional regulation on a genome-wide level. Here, we use two closely related nematode species to perform a global comparison of mRNA and protein abundance throughout the entire life cycle from embryogenesis to adulthood of a metazoan organism.

The nematodes *C. elegans* and *C. briggsae* are particularly attractive model organisms due to their highly reproducible development (Sulston et al., 1983; Zhao et al., 2008). The two species evolved from a common ancestor about 30–50 million years ago (Stein et al., 2003; Cutter, 2008) and are strongly diverged on the sequence level ($K_S = 1.78$ and $K_A = 0.11$) (Stein et al., 2003). Given that every neutral site in the genome should be substituted on average 1.78 times, a scenario of neutral evolution without any purifying selection would imply the loss of common regulatory sequences and reduce conservation of expression changes to background levels. However, despite the relatively long evolutionary distance, morphology, body plan and development of the two nematodes remained strikingly similar throughout the lifecycle. Even cell lineages are almost completely conserved (Zhao et al., 2008). Comparing developmental gene expression changes in the two nematodes will therefore help to elucidate the permitted evolutionary variability of gene expression that leaves the morphology and physiology of a species largely unaffected.

To quantify fold changes for thousands of proteins between defined developmental stages in both species, we used stable isotope labeling by amino acids combined with mass spectrometry. To perform a genome-wide comparative analysis of the evolution of transcript and protein abundance during
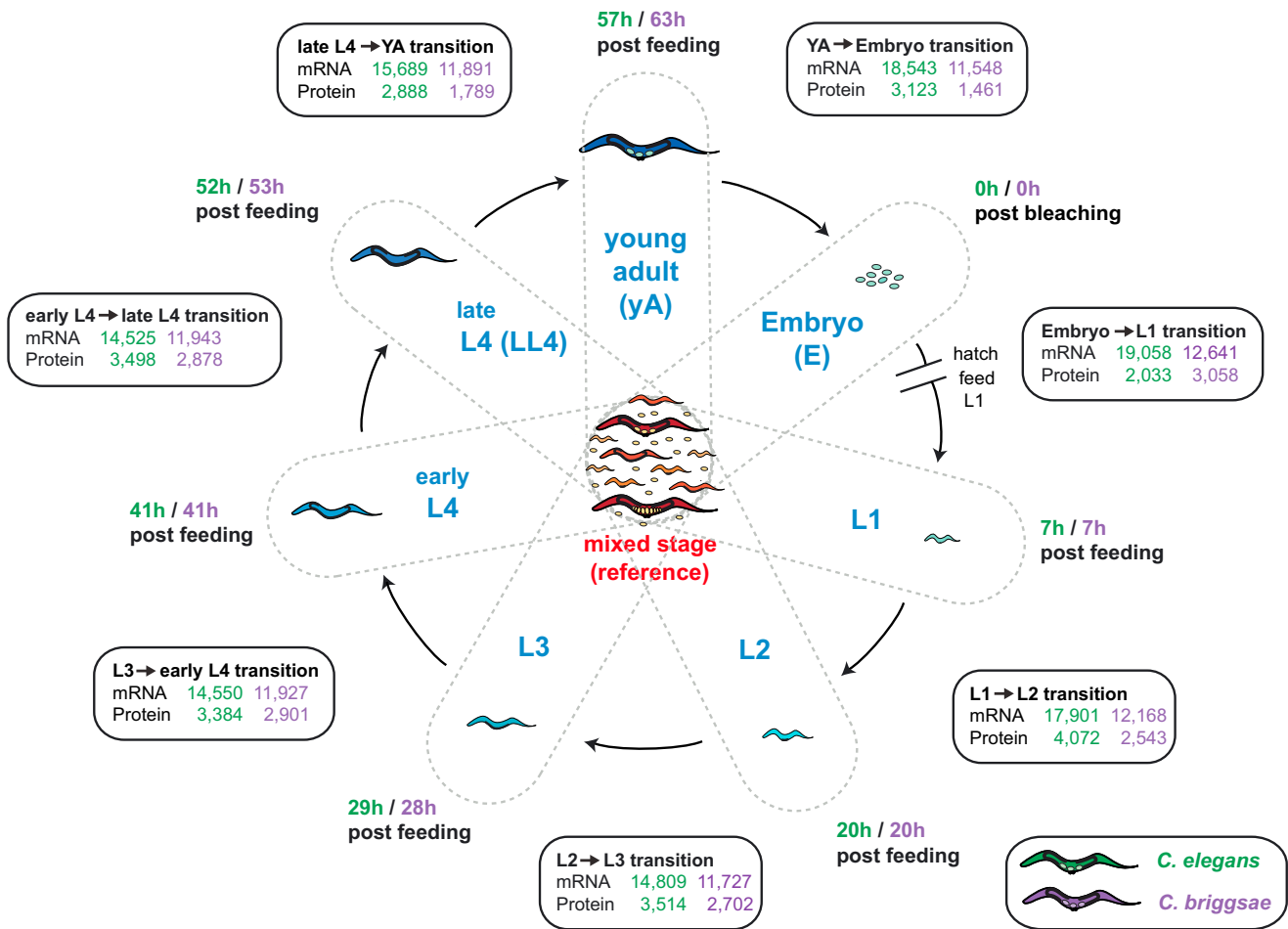
Figure 1. Nematode Life Cycle and Timing of Samples Used for Protein and Transcript Quantification

Experimental setup and time line for generation of *C. elegans* and *C. briggsae* samples for mRNA sequencing and mass spectrometry. Light-labeled synchronized worms (blue) were harvested at each stage (hours after feeding synchronized L1 larvae). A nonsynchronous heavy-labeled sample (red), containing a mixture of all time-contiguous stages, was used as a reference sample. For mRNA sequencing, all samples were analyzed independently. In order to quantify protein fold changes against the reference sample as SILAC ratios, each of the staged samples was mixed 2:1 with the reference sample. Numbers in the boxes represent quantified transcripts and proteins for each stage transition (*C. elegans*, green; *C. briggsae*, purple).

development, we complemented our protein data with mRNA quantification by mRNA sequencing. We observed that the degree of conservation is almost exactly the same for protein and transcript expression changes. Moreover, differences in protein and mRNA fold changes for the same gene were also conserved, preferentially if transcript changes were larger than protein changes, i.e., were buffered on the protein level.

We used our data to identify a pathway with accelerated evolution of expression changes and attempted to reproduce the observed cross-species changes within a single species by perturbation experiments.

RESULTS

Measuring Transcript and Protein Abundance in Parallel throughout Development

We sought to compare the developmental transcriptomes and proteomes of *C. elegans* and *C. briggsae* at well-defined develop-

mental stages covering the entire life cycle (Figure 1). The currently most accurate way to quantify changes in protein levels is stable isotope labeling and mass spectrometry (Heck and Krijgsveld, 2004), combining and coanalyzing differentially labeled samples. SILAC (stable isotope labeling with amino acids in cell culture) employs metabolic incorporation of heavy stable isotope-containing amino acids (Ong et al., 2002). The method was originally developed in cell culture and subsequently extended to several metazoan model organisms, including *C. elegans* (Krüger et al., 2008; Looso et al., 2010; Sury et al., 2010; Fredens et al., 2011; Larance et al., 2011). We generated SILAC worms by feeding worms on *E. coli* labeled with heavy lysine (Figure 2A; Supplemental Experimental Procedures). We did not observe any apparent difference between light and heavy worms (assessed by phenotype, developmental time, and number of worms obtained, n > 1,000). Efficient incorporation of heavy lysine was already observed in F1 adult worms (95% heavy-labeled peptides), with virtually complete labeling in F2 adult worms (99.5% heavy peptides).
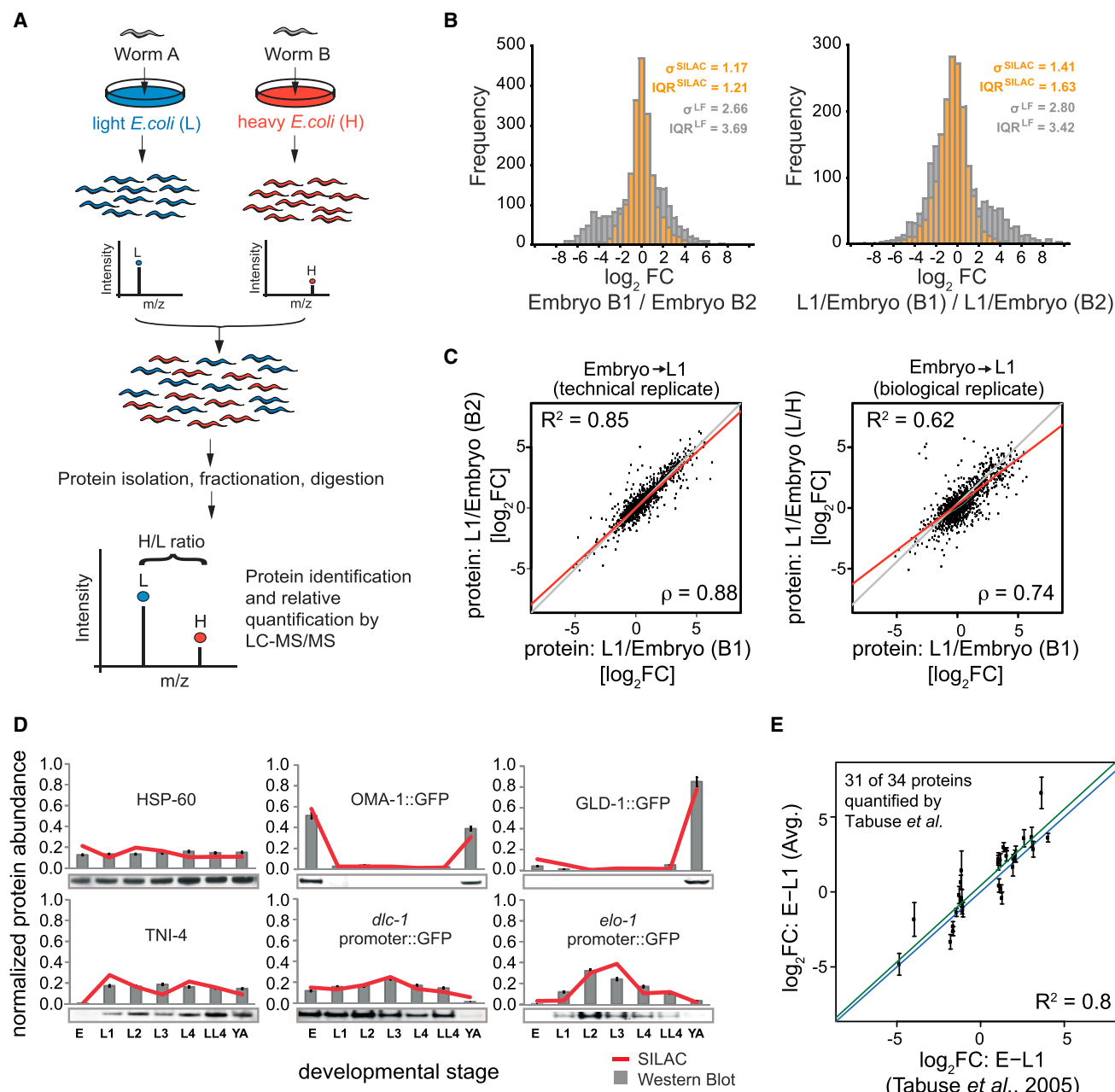
Figure 2. The SILAC Worm

(A) Stable isotope labeling with amino acids in nematodes. Nematodes are fed with either light- (L) or heavy- (H) labeled *E. coli* for at least two generations. Samples H and L are mixed at a defined ratio before processing and analysis by LC-MS/MS. Pairs of identical peptides with different stable-isotope compositions can be distinguished based on their mass difference. The ratio of peptide intensities reflects differences in protein abundance.

(B) Precision of label-free versus SILAC-based protein quantification. Two technical replicates of 1:1 mixtures were quantified based on intensity values (label-free, LF; gray) or based on SILAC ratios (SILAC; orange). SD (σ) and interquartile range (IQR) are shown for two replicates of the embryonic stage versus reference (left) and of the embryo-L1 fold changes (right).

(C) Pearson's R^2 and Spearman's correlation (ρ) between SILAC replicates of embryo-L1 log$_2$-fold changes for technical (left) and biological (right) replicates (see Supplemental Experimental Procedures for description and nomenclature of replicates).

(D) Validation of SILAC-based protein abundance by western blotting using antibodies for selected proteins, prepared from independent biological replicate samples and normalized against tubulin (TBA-2).

(E) Validation of SILAC-based embryo-L1 protein fold changes, averaged across biological replicates, by 2D difference gel electrophoresis (Tabuse et al., 2005). Error bars indicate the SD across replicates; the blue line represents the diagonal. A regression (green line) yields $R^2 = 0.8$.

See also Figure S1.

We collected carefully staged unlabeled (light) worms of all major developmental stages (Figure 1; Supplemental Experimental Procedures) and combined these samples with a heavy SILAC reference sample (~99.5% heavy peptides) of asynchronously cultured worms, comprising a mixture of all time-contiguous developmental stages and serving as a common internal standard for the mass spectrometry runs (Figures 1 and 2A). For fold change quantification, we used revised high-quality gene models in *C. elegans* (Gerstein et al., 2010) comprising 21,774 genes and produced ab initio transcript annotations for *C. briggsae*. Our *C. briggsae* gene models were inferred based on sequencing read coverage, and we only maintained annotations supported by an alignment of *C. elegans* protein coding exons (Supplemental Experimental Procedures). This strategy yielded 13,938 *C. briggsae* orthologs. We note that our gene models largely overlap with a recently published annotation (Uyar et al., 2012). Of the 13,355 one-to-one orthologs based on reciprocal best protein blast alignments of these gene models to our *C. elegans* annotation, 12,008 (90%) correspond to orthology relations in our *C. briggsae* annotation. The respective gene models are highly overlapping: the sequence of 86% of the genes overlaps more than 80% between both annotations.

In total, we quantified 9,162 (5,552) proteins in *C. elegans* (*C. briggsae*) at a false discovery rate of 5%. In our hands, quantification based on the heavy SILAC reference was at least 2-fold more precise than label-free (LF) quantification according to a benchmark test ($\sigma^{SILAC} = 1.17$, $\sigma^{LF} = 2.66$; Figure 2B) and SILAC ratios reflect true protein fold changes inferred from mixing experiments (Figures S1A and S1B). Moreover, fold change variability across technical replicates was low (Spearman's rank coefficient $\rho = 0.88$) and increased slightly for biological replicates ($\rho = 0.74$), indicating moderate noise due to actual variation in protein abundance, a lack of timing precision or variable labeling efficiency for lowly expressed proteins (Figures 2C, S1E, and S1F). We first successfully validated the protein fold changes that we computed from in vivo SILAC by western blots for 20 proteins (Figures 2D, S1G, and S1H). Moreover, fold changes of 31 proteins measured by 2D gel electrophoresis (Tabuse et al., 2005) correlated strongly with our computed protein fold changes ($R^2 = 0.8$, Figure 2E).

We complemented our proteome data with transcript quantification by RNA sequencing (RNA-seq) of polyadenylated transcripts in the same biological samples. We obtained reliable expression for 19,549 (12,836) genes in *C. elegans* (*C. briggsae*) (Figures S1C and S1D; Table S1).

We validated our RNA-seq data, using quantitative RT-PCRs (qRT-PCRs) for 14 randomly selected genes covering the entire dynamic range of observed expression values, and measured a high correlation to RNA-seq-derived expression ($R^2 = 0.8/0.85$ for *C. elegans*/*C. briggsae*, Figure 3A). Moreover, reproducibility across biological replicates was high ($\rho > 0.82$, Figures S2A and S2B).

To examine how well our discrete set of developmental stages reflects transcript expression in our contiguous reference sample, we attempted to reproduce the composition of the reference sample by a mixture of all staged samples in silico. To this end, we defined for each developmental stage a vector with transcript expression of all *C. elegans* genes and computed the linear combination of these vectors that best matches the expression vector for the reference sample by a multilinear regression. This in silico mixture reproduces the reference sample almost as good ($R^2 = 0.92$) as a true technical replicate ($R^2 = 0.93$). Contribution of each sample is essential because repeating the regression without, for instance, the young adult sample reduces the correlation ($R^2 = 0.81$, Figure 3B). Moreover, the optimized weights of the in silico mixture reflect the estimated contribution of the respective stage (determined by microscopy, n > 1,000) to the reference sample (Figure 3C). The in silico mixture for *C. briggsae* reproduces our composition estimates based on microscopic imaging equally well (Figure S2C). Developmental transcript expression changes are thus reflected by expression changes between our staged samples for the vast majority of genes.

In Figure 3D, examples are shown for a gene with conserved transcript and protein abundance, but differential embryo-L1 fold changes (*rpl-9*) and for a gene with nonconserved expression changes (*syd-2*).

A direct comparison of protein and transcript embryo-L1 fold change variability between biological replicates indicates that the level of noise is increased for protein quantification (Figure 3E). On average, the fold change error was comparable across the entire dynamic range (~0.5 for proteins versus ~0.25 for mRNAs), with slightly bigger errors for larger fold changes.

We supply transcript expression and SILAC protein ratios for all developmental stages in *C. elegans* and *C. briggsae* in Table S2, and graphical representations of expression profiles can be screened on our publicly available online database at http://elegans.mdc-berlin.de.

Transcript and Protein Abundance Changes Substantially during the Nematode Life Cycle

We first investigated temporal dynamics of transcript and protein abundance throughout *C. elegans* development. On both levels, pairs of larval stages were most highly correlated in comparison to pairs involving the young adult (YA) or the embryonic (E) stage (Figures 4A, 4B, and S3A). Therefore, transcript and protein abundances are relatively uniform throughout larval development and undergo pronounced changes at the embryo to larval transition and after completion of the final larval stage upon onset of oogenesis (Figure S3B).

Then, we assessed to what extent transcript expression changes explained protein abundance changes. Strikingly, only modest correlation was observed for the embryo-L1 ($\rho = 0.41$), the late L4 young adult ($\rho = 0.30$), and the young adult-embryo transition ($\rho = 0.17$) and almost no correlation at larval transitions ($\rho \sim 0$) (Figures 4C and S3). The pronounced differences between transcript and protein abundance changes suggest ubiquitous regulation at the posttranscriptional level.

Clustering of Temporal Expression Profiles Reveals Broad Posttranscriptional Regulation

We next searched for groups of genes with similar expression profiles throughout *C. elegans* development and analyzed to
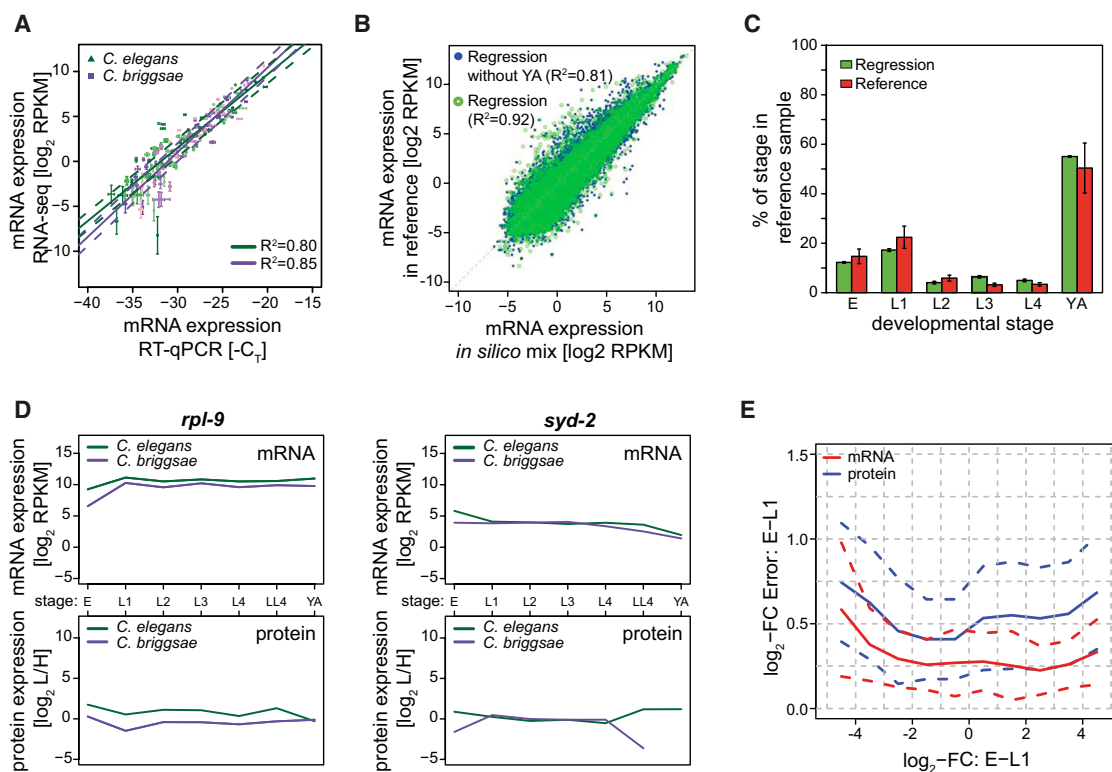
Figure 3. Validation of Transcript and Protein Quantification

(A) Validation of RNA-seq data by qRT-PCR for 14 genes with differential expression across development. Shown is the regression between $\log_2$RPKM and $-C_T$. The broken lines represent a 2-fold interval around the regression line. Different shadings of green (*C. elegans*) and purple (*C. briggsae*) correspond to distinct developmental stages from embryos (dark) to young adults (light). Error bars represent the SD across replicates.

(B) Correlation between transcript expression in the reference sample and an in silico mixture of all stages (green circles) and after omitting the young adult sample (blue points).

(C) Comparison of the fraction of total mRNA from each stage in the reference sample as computed by the in silico mixture to estimates based on microscopic analysis for *C. elegans* (n > 1,000). Error bars indicate the error of the regression coefficients and the uncertainty of our estimates, respectively.

(D) Temporal expression profile for transcripts and proteins of the ribosomal gene *rpl-9* (left), which correlates well between the two species at all stages, and the gene *syd-2* (right), which shows divergent expression changes in the two species at the embryo-L1 transition.

(E) Variability of transcript (red) and protein (blue) $\log_2$-fold changes quantified by the SD across biological replicates as a function of the fold change magnitude. Shown are the average (solid line) and the SD (broken line) of the variability across all genes.

See also Figure S2.

what extent transcript and protein level changes correlated within these groups. Hierarchical clustering of temporal expression profiles for all genes with quantified protein abundance for at least three developmental stages (Supplemental Experimental Procedures) yielded seven distinct expression clusters (Table S3A; Figure S3C). Four of those exhibited un- or even anticorrelated transcript and protein fold changes at the embryo-L1 transition, suggesting that posttranscriptional control modifies protein levels for a large fraction of genes. Next, we performed the same clustering procedure for *C. briggsae* (Table S3B; Figure S3D) and found that expression profiles in the two species looked similar and that the cluster composition was highly conserved (Table S3C). Hence, the majority of genes display conserved expression profiles.

As supplementary information, we computed enrichment of RNAi phenotypes (Table S3D; Supplemental Experimental Procedures) and identified overrepresented gene ontology

(GO) terms using the DAVID functional annotation tool (Huang et al., 2009; Table S4). For instance, the functional analysis reveals a strong enrichment of diverse developmental phenotypes (Table S3D) and developmental functions (Table S4) among genes with increased transcript and protein abundance in embryos (cluster 4 in Figure S3C). Metabolic functions, on the other hand, were enriched among genes upregulated on the transcript and protein level during larval development and adulthood (cluster 1 in Figure S3C).

Evidence for Oscillating Expression of Genes with Large Expression Changes at Larval Transitions

Many genes with highly dynamic transcript expression during larval development were discarded from clustering due to the lack of protein quantification. In *C. elegans*, these genes appear as a distinct population with strongly increased
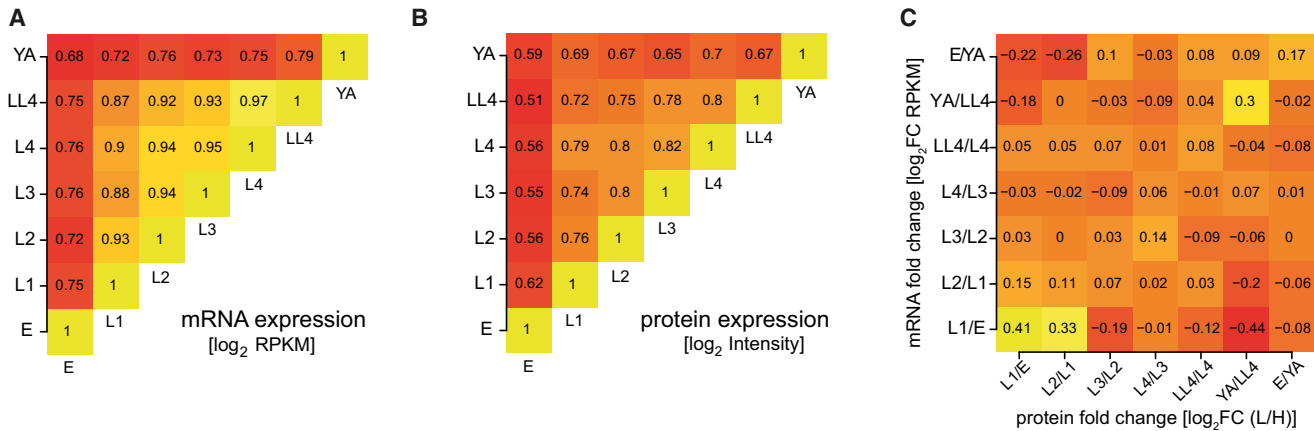
Figure 4. Correlation of Transcript and Protein Abundances Varies between Developmental Stages
The heatmaps indicate correlation between log$_2$-expression of transcripts (A) and proteins (B) for all possible pairs of stages. Protein abundance was quantified by normalized protein intensities. (C) Correlation between transcript and protein fold changes (measured by SILAC). See also Figure S3.

expression at the L3 stage and correlated temporal expression changes throughout development (Figures 5A and S4). To analyze the behavior of this group of 866 genes in more detail, we measured the expression of eight randomly selected candidates and five controls by qRT-PCRs in a 3 hr time course throughout *C. elegans* and *C. briggsae* development. Strikingly, we measured oscillating expression of these genes synchronized with larval transitions in both species (Figure 5B), whereas control genes remained overall uniformly expressed (Figure 5C). Given that oscillating expression could be validated for all eight randomly selected candidates, the majority of the 866 genes presumably show conserved expression oscillations in the two nematodes. Upon each larval transition, nematodes, like all ecdysozoans, replace their exoskeleton in a process called molting (Page and Johnstone, 2007). Noticeably, we found a 6-fold overre-presentation of molting phenotypes (Frand et al., 2005) among our cycling genes (p < 7*10^{-7}). We note that a large number of genes oscillating throughout *C. elegans* larval development were independently discovered while this manu-script was submitted (Kim et al., 2013). However, evolutionary conservation of oscillatory expression was not addressed in this study. We compared our dynamically expressed genes to the 1,592 genes within oscillating clusters identified by Kim et al. and found that 497 out of the 866 candidates (57%) fall into one of these clusters (p = 0, hypergeometric test), which confirms that most of our candidates were truly oscillating.

Because we quantified protein abundance at more than three stages for only 99 out of the 866 genes, we could not reliably address the dynamics of protein expression. We note, however, that the average SILAC ratio of these proteins varies up to 2-fold between different larval stages (data not shown) suggesting dynamic regulation also on the protein level.

In summary, we discovered numerous genes with conserved oscillating mRNA levels during larval development that are enriched in molting phenotypes.

Transcript and Protein Fold Changes at the Embryo-to-Larva Transition Are Conserved

To further investigate evolutionary conservation of gene expression throughout development, we computed the cross-species correlation of mRNA and protein abundance changes at each developmental transition (Figures S5A and S5B). Both mRNA and protein fold changes correlated most strongly at the embryo-L1 transition (Spearman's correlation coefficient ρ > 0.62 [mRNA]/0.65 [protein]; Figure S5A). It has been postulated that gene expression is more evolutionarily constrained in developing animals compared to adults (Kalinka et al., 2010). However, we also observed well-conserved fold changes at the late L4 young adult transition (ρ = 0.59/0.24; Figure S5A) and speculated that these changes originate primarily from the germline, induced by the initiation of oogenesis. Analyzing transcript expression changes of germline enriched and somatic genes (Supplemental Experimental Procedures) separately revealed that these groups largely correspond to genes up- and downregulated in young adults versus late L4 larvae, respectively (Figures S5C and S5D). Hence, the well-conserved transcript fold changes at this transition are most likely induced by a conserved gene expression program in the maturing germline.

To evaluate cross-species conservation of transcript and protein fold changes comprehensively, we focused on the embryo-L1 transition, because synchronization at these stages was most reliable. We first tested if strong expression changes, i.e., transcript or protein fold changes exceeding the average fold-change variability (SD of log$_2$-fold changes), were conserved. About 15% (19%) of all genes display strong transcript (protein) expression changes with the same direction in both species, whereas only 0.7% (0.6%) of transcripts (proteins) change in opposite directions (Figure 6A). Hence, evolutionary reversion of strong expression switches is rare, and the on- or off-state of a gene is therefore well conserved.

Next, we examined conservation of fold change magnitudes. To correct for different levels of expression noise in transcript and protein quantification, we normalized by the average fold change variability. Interestingly, the majority of transcripts (68%)
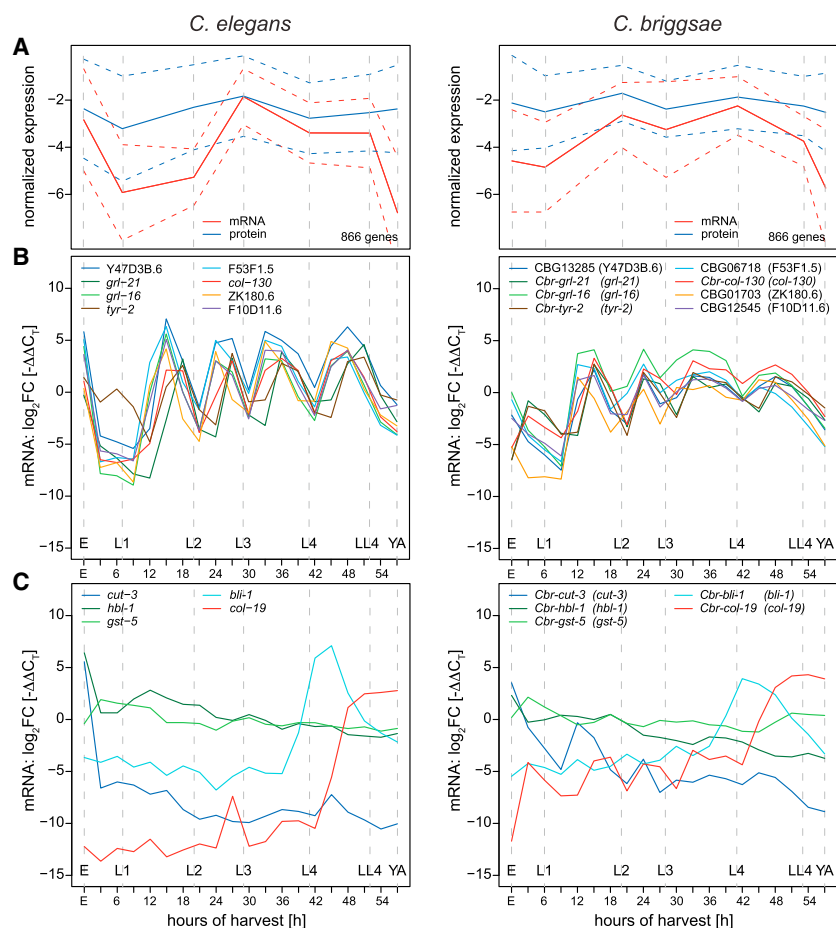
Figure 5. Transcriptome Analysis Reveals Genes with Cycling Expression

(A) Clusters of genes with dynamic expression during larval development in *C. elegans* (left) and *C. briggsae* (right). The average expression (solid line) and the SD (broken line) are shown.

(B) qRT-PCR of eight randomly selected genes for a 3 hr time series covering the entire development from embryo to young adult.

(C) qRT-PCR of five control genes with constant expression according to our data for a time series covering the entire development from embryo to young adult with samples taken every 3 hr. In (B) and (C), Y57G11C.34 was used as internal control for *C. elegans* and *Cbr-ero-1* for *C. briggsae*; $\Delta\Delta C_T$ was computed by comparing to expression in the reference sample.

See also Figure S4.

scripts and proteins was found to be comparable across the entire dynamic range.

Next, we compared conservation of the fold change magnitude. We considered a transcript or protein fold change magnitude as conserved, if the variability intervals of the respective fold changes, inferred from the SD across biological replicates, overlapped between the two species (Figure S5E). We computed the fold enrichment of conserved genes above the background level obtained with shuffled orthology assignments of genes in the two species. We observed comparable fold enrichments for transcripts (2.02-fold) and proteins (2.05-fold), confirming a similar degree of conservation on both levels at the embryo-L1 transition (Figure 6D). Thus, conservation of expression changes between both species is twice as high as expected by chance and surprisingly similar for transcripts and proteins, indicating that protein levels are not, on average, under stronger evolutionary constraint than mRNA levels.

Conservation of Posttranscriptional Regulation Is Enhanced if Transcript Fold Changes Are Dampened on the Protein Level

The lack of correlation between mRNA and protein level changes throughout development (Figure 4C) in each species suggests that protein abundance is controlled by substantial regulation on the posttranscriptional and/or (post)translational level, hereafter summarized as posttranscriptional regulation. To investigate evolutionary conservation of this component, we split the ensemble of all *C. elegans* genes into groups with up- and downregulated transcripts at the embryo-L1 transition and subdivided these groups into genes whose protein fold changes exceed their transcript fold changes (amplifying posttranscriptional regulation), and genes whose protein fold changes buffered their transcript fold changes (dampening posttranscriptional regulation). To assess evolutionary conservation, we computed the fraction of *C. briggsae* genes that fall into the same subgroup
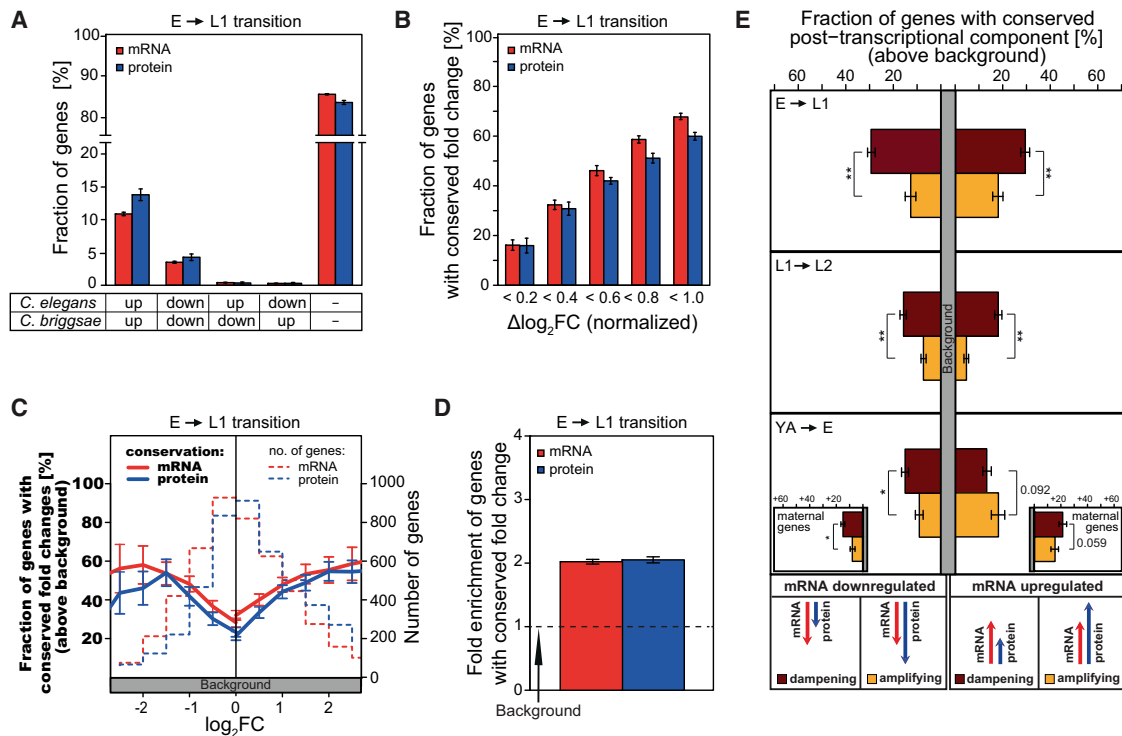
and proteins (60%) have a fold change variability of less than 2-fold (Figure 6B). Taken together, the data suggest that evolution only permits a limited degree of expression variability between morphologically and physiologically similar organisms.

Similar Conservation of Transcript and Protein Fold Changes at the Embryo-to-Larva Transition

Because proteins are the mediators of biological functions, whereas mRNAs are frequently considered only as coding intermediates, protein abundance could potentially be more highly conserved than transcript expression. We tested this hypothesis at the embryo-L1 transition by analyzing conservation of a given degree of up- or downregulation for transcripts or proteins. We extracted all *C. elegans* genes exceeding a given positive fold-change threshold and computed the fraction of genes with fold changes higher than the same threshold in *C. briggsae*. This fraction corresponds to the conservation probability of a given degree of upregulation. The conservation probability for downregulation was calculated accordingly (Figure 6C). To correct for expression noise, we subtracted the conservation probability obtained with shuffled orthology relations between genes in *C. elegans* and *C. briggsae*. For transcripts and proteins, the conservation probability above noise increases up to ~50% for 4-fold expression changes (Figure 6C). Conservation of tran-

Figure 6. Cross-Species Comparison of Transcript and Protein Fold Changes at the Embryo-L1 Transition between *C. elegans* and *C. briggsae*

(A) Fraction of genes with conserved and nonconserved pronounced up- or downregulation, exceeding the fold change SD for proteins (3.0-fold) or transcripts (4.2-fold). Error bars are based on random counting statistics.

(B) Fraction of genes with a maximum $\log_2$-fold-change difference between *C. elegans* and *C. briggsae* after normalizing fold changes by the SD to account for different dynamic ranges of transcript and protein fold changes. Error bars indicate the SE inferred by bootstrapping.

(C) Fraction of genes with conserved minimal up- or downregulation. For all genes with a fold change higher (right) or lower (left) than a given threshold in *C. elegans*, the fraction of genes with a fold change higher or lower than the same threshold in *C. briggsae* was computed. Background conservation has been subtracted. Error bars are based on random counting statistics.

(D) Fold enrichment of genes with strictly conserved transcript or protein fold change magnitudes, measured by overlapping intervals of variability. Error bars indicate the SE inferred by bootstrapping.

(E) Fraction of genes with a conserved posttranscriptional fold change component. For all *C. elegans* genes with a positive (negative) $\log_2$-fold difference between protein and transcript fold changes, the fraction of genes with a positive (negative) $\log_2$-fold difference in *C. briggsae* was computed. Background conservation has been subtracted. Conservation is shown for up- and downregulated transcripts with dampening and amplifying posttranscriptional regulation. The inset displays the conservation for maternal genes only. Error bars are based on random counting statistics (*p < 0.05, **p < 0.001).

See also Figure S5.

like in *C. elegans*. After subtracting background conservation obtained for shuffled orthology relations, conservation increased up to 30% (Figure 6E). These data provide evidence that post-transcriptional control is highly conserved during metazoan development. Conservation is significantly enhanced for genes subject to posttranscriptional dampening, whereas amplifying changes are less well conserved.

In contrast, we observed that dampening and amplifying post-transcriptional regulation were equally well conserved at the young adult-to-embryo transition for transcripts upregulated in embryos. The embryonic transcriptome is composed of maternal genes and zygotic genes that are transcribed by the embryo after zygotic genome activation. We tested if maternal and zygotic genes (see Supplemental Experimental Procedures; Table S5) have different conserved modes of posttranscriptional regulation. We observed that dampening regulation of maternal mRNAs was more highly conserved than amplifying regulation (Figure 6E),

whereas zygotic mRNAs displayed enhanced conservation of amplifying posttranscriptional regulation (Figure S5F).

In summary, we find that strong positive and negative transcript expression changes are dampened by posttranscriptional regulation, potentially enforcing robust protein levels throughout longer developmental timescales. In the embryo, however, we observe preferential conservation of amplifying posttranscriptional gene regulation of genes transcribed in the embryo, which may be essential to ensure fast accumulation of crucial regulators of embryogenesis.

Fold Change Conservation at the Embryo-L1 Transition Coincides with Conservation of Exonic and 3' UTR Sequence

To compare conservation of mRNA and protein fold changes to conservation of regulatory sequence at the embryo-L1 transition, we downloaded three-way alignments of *C. elegans*,

C. briggsae, and *C. remanei* from the UCSC genome browser (Dreszer et al., 2012). We extracted alignments for promoter sequences (1 kb upstream), for 3′ UTRs (Mangone et al., 2010) and for all exons. We only considered mRNAs and proteins, which change at least 2-fold at this transition in *C. elegans* and assessed conservation of up- or downregulation in *C. briggsae.* We then compared sequence conservation of genes with conserved and nonconserved fold changes. We also included genes with a conserved posttranscriptional component into this comparison (Figure S5G). Genes with conserved mRNA fold changes do not display significantly increased sequence conservation. Genes with conserved protein fold changes, on the other hand, are overall significantly more conserved and, in particular, have more highly conserved 3′ UTRs, suggesting enrichment in binding sites for RNA binding proteins or microRNAs. Genes with conserved posttranscriptional component also have more highly conserved exons and 3′ UTRs, with the only exception of downregulated transcripts subject to dampening regulation. However, among the nonconserved genes in this group are 125 genes with conserved but only 36 genes with nonconserved protein fold changes, explaining the high sequence conservation.

In summary, the observed patterns of conservation of expression fold changes are consistent with trends in sequence conservation.

Increased Evolutionary Fold Change Variability Identifies a Putative Target of Adaptive Evolution

Finally, we searched for classes of genes with strongly reduced or enhanced fold change conservation. Regulatory factors are presumably well conserved, because mutations of *trans*-acting factors can affect whole gene networks. We extracted a list of transcription factors from the literature (Haerty et al., 2008) and analyzed evolutionary variability of their expression changes at the embryo-L1 transition. The 761 (44) transcription factors with measured transcript (protein) expression changes show significantly less cross-species fold change variability than random sets of genes. On the transcript (protein) level, we observed a 16% (33%) reduction (Figure S6A), consistent with enhanced sequence conservation of transcription factors (Haerty et al., 2008).

Next, we explored genes with reduced fold change conservation and validated a subset of these by qRT-PCRs (Figure S6B). Among those were genes involved in an insulin/insulin-like growth factor (IGF) signaling pathway. The main downstream target of this pathway, DAF-16, is a deeply conserved FOXO-family transcription factor regulating lifespan in flies, worms, and mammals (Tatar et al., 2003). Strikingly, we observed a 4-fold reduction of *daf-16* transcript expression, aggregated across all isoforms, in *C. briggsae* embryos compared to *C. elegans* embryos, whereas larval expression was comparable in both species (Figure S6C). We successfully validated RNA-seq-based embryo-L1 fold changes by qRT-PCR for *daf-16* and four additional differentially regulated genes (*daf-12*, *daf-7*, *syd-2*, *ttr-1*), which are known DAF-16 targets (Figure 7A). We did not detect DAF-16 at the protein level in our mass spectrometry (MS) analysis, perhaps due to relatively low abundance. Therefore, to quantify DAF-16 protein levels, we used a poly-

clonal antibody directed against the C-terminal region of the protein, which is shared by all known isoforms and highly conserved in both species (78% amino acid identity). Western blotting indicated that DAF-16 protein levels are reduced in *C. briggsae* embryos compared to *C. elegans* (Figure 7B), whereas protein abundance increases in both species at the embryo-L1 transition to comparable level. Together, with the observation that mRNA levels remain unchanged at this transition in *C. elegans*, these data suggest amplifying posttranscriptional regulation of *daf-16*. To which degree the difference between mRNA and protein fold changes has evolved cannot be reliably assessed, given that the western method is not quantitative enough to determine precise fold changes. In any case, our data clearly suggest that differences in embryonic *daf-16* mRNA expression and protein abundance have evolved between both species. Next, we extracted a list of 446 predicted DAF-16 targets from the literature (Murphy et al., 2003). For these genes, we observed significantly increased evolutionary variability of transcript and protein fold changes in comparison to random sets of genes ($p < 0.001$, Figure 7C). To test whether this increase is driven by *daf-16*, we performed an RNAi-mediated knockdown of *daf-16* in *C. elegans* embryos (Figure 7D) and globally measured protein fold changes compared to wild-type L1 larvae. Interestingly, after knockdown of *daf-16* in *C. elegans*, protein fold changes at the embryo-L1 transition were slightly more correlated to *C. briggsae* (R^2_{RNAi} = 0.50 versus $R^2_{control}$ = 0.47). Consistently, the distribution of residuals was shifted significantly ($p < 0.004$) to lower values for the *daf-16* knockdown versus the control sample (Figure 7E). Hence, the *daf-16* knockdown overall reduces the cross-species variability. Moreover, reduced expression of *daf-16* in *C. briggsae* embryos explains a fraction of the global proteome changes between the two species. To investigate whether the set of predicted DAF-16 targets accounts for this observation, we compared the difference in embryo-L1 log_2-fold changes between control and *daf-16* knockdown samples to the difference between *C. elegans* and *C. briggsae* wild-type samples. If both numbers were either positive or negative for a given gene, the cross-species fold change modulation is consistent with differential expression of *daf-16*. In contrast to the ensemble of all genes, with equal numbers of consistent and inconsistent fold changes, DAF-16 targets comprise almost twice as many consistent as inconsistent fold changes (Figure 7F). We could reproduce these observations with an independent biological replicate (Figures S6D–S6F). These data suggest that the enhanced expression divergence of DAF-16 targets is likely a result of differential expression of *daf-16* itself and that the *daf-16* regulatory network is a possible target of adaptive evolution.

DISCUSSION

In this study, we investigated joint dynamics and evolutionary conservation of transcript and protein abundance during development of a well-studied metazoan model organism on a genome-wide scale. Only a handful of studies have quantified developmental protein fold changes in *C. elegans* on a large scale, either using 2D-gel electrophoresis (Tabuse et al., 2005) or metabolic ^{15}N labeling combined with mass spectrometry
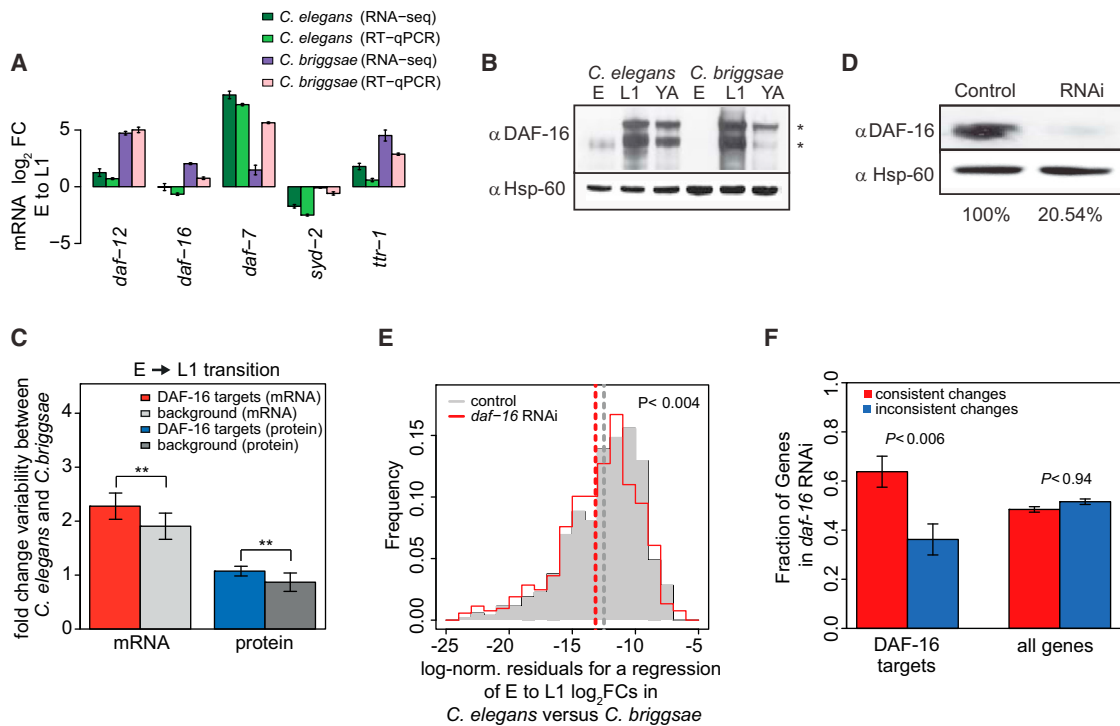
Figure 7. Identification of a Pathway with Enhanced Expression Divergence at the Embryo-L1 Transition

(A) Validation of RNA-seq-based quantification by qRT-PCR for *daf-16* and four known DAF-16 targets with diverged expression changes between *C. elegans* and *C. briggsae* at the embryo-L1 transition. qRT-PCR was performed for individual biological replicate samples. Error bars represent the SD across replicates (n ≥ 3).

(B) Western blot analysis of DAF-16 protein abundance in *C. elegans* and *C. briggsae* embryos (E), L1 larvae (L1), and young adults (YA). Hsp-60 was used as loading control and for normalization. *Multiple bands represent expression of DAF-16 isoforms.

(C) Average of the absolute $\log_2$-fold-change difference between *C. elegans* and *C. briggsae* for DAF-16 targets and random groups of nontargets. Mean and SE are inferred by bootstrapping (**p < 0.001).

(D) Western blot analysis of DAF-16 after RNAi-mediated knockdown of *daf-16*. Protein knockdown was quantified as a percentage of the control (set as 100%). Hsp-60 was used as a loading control and for normalization.

(E) Distribution of the logarithm of squared normalized residuals from a regression of protein $\log_2$-fold changes between *C. elegans* and *C. briggsae*. Upon knockdown of *daf-16* in *C. elegans* embryos, the distribution (red line) is shifted compared to a control transfection (gray) (p < 0.004, Wilcoxon rank sum test).

(F) Genes with differences in $\log_2$-fold changes between *daf-16* knockdown and control *C. elegans* embryos that exhibit consistent (red) or inconsistent (blue) differences between *C. elegans* and *C. briggsae*. Data are shown for all genes and for the subset of predicted DAF-16 targets (Murphy et al., 2003). Error bars are based on random counting statistics. A hypergeometric test was performed to assess an enrichment of consistent fold changes.

See also Figure S6.

(Geillinger et al., 2012), and these studies were limited to a fold-change determination for a few hundred proteins. Tabuse et al. (2005) measured expression changes for a small number of proteins at the embryo-to-L1 transition and the fold change magnitude compares very well to our data ($R^2 = 0.8$; Figure 1E).

Evolution of transcript expression during *Caenorhabditis* embryogenesis was previously investigated in great detail (Levin et al., 2012), and, while our study was under review, a comparison of transcript expression and translation rate changes at a specific developmental transition was published (Stadler and Fire, 2013). Stadler et al. used ribosome profiling to compare changes in ribosome occupancy to transcript expression changes upon the L1 diapause exit. In contrast to protein quantification by mass spectrometry, however, this approach only reveals changes in ribosome association of mRNAs, not protein abundance changes, which are also affected by (post)translational modifications. Nonetheless, this study also

provides evidence for important posttranscriptional regulation at a different developmental transition.

We focused on the embryo-L1 transition to examine general properties of posttranscriptional versus transcriptional regulation. For most genes, protein abundance changes could not be explained by changes of the transcript level, suggesting ubiquitous posttranscriptional regulation that could be exerted by factors such as microRNAs or RNA binding proteins or a consequence of enzymatic protein modifications directly effecting protein levels.

At this transition we could also directly compare evolutionary conservation of transcript and protein fold changes. In previous studies, enhanced conservation of protein versus transcript abundance was derived for mixtures of homogenized whole animals of various developmental stages (Schrimpf et al., 2009; Weiss et al., 2010). In contrast, our analysis suggests that transcript and protein fold changes are conserved to a very similar

degree. In order to arrive at this conclusion, we had to account for different levels of technical noise in protein and mRNA quantification. To address a possible ascertainment bias in our conservation measurements due to a selection of specific genes by our *C. briggsae* annotation, we computed fold change conservation of one-to-one orthologs inferred from recently published *C. briggsae* gene models (Uyar et al., 2012). This annotation was highly similar to our own gene models, and fold change conservation was invariant (Figures S5H and S5I).

Our finding implies that regulation on the level of mRNA and protein is of similar functional importance during metazoan development. This may seem surprising given that proteins are the functional products of most genes. However, posttranscriptional regulation presumably modulates protein levels produced from invariant mRNA levels in a developmental stage- or condition-specific way. The mRNA fold change as primary input for protein production is therefore read out in a context-dependent way and hence presumably under equally strong evolutionary constraint as the protein fold change.

Our results further include that the fold change magnitude of mRNAs and proteins is remarkably well conserved during ~30 million years of evolution separating the two nematodes. Therefore, not only the on- or off-state of a gene and the architecture of the regulatory circuits appear to be exposed to selective pressure, as postulated for gene regulatory networks during metazoan embryonic development (Peter and Davidson, 2011), but also the precise level of temporal up- or downregulation between developmental stages.

The posttranscriptional component of protein fold changes was also well conserved, in particular, if transcript fold changes were dampened on the protein level. We cannot rule out that this observation is partially due to technical reasons such as systematic underestimation of protein fold changes. However, predominance of amplifying regulation for zygotically transcribed genes and our SILAC mixing experiments argue against this possibility. Hence, gene regulation at the posttranscriptional level is ubiquitous and functionally relevant during animal development, in particular, when protein fold changes are buffered. Furthermore, it is thought that for microRNAs and most RNA binding proteins, which bind 3′ UTRs of mature mRNAs, the regulatory effect on translation is negative.

Finally, we used our data to screen for pathways that could be a target of adaptive evolution. Among genes with enhanced cross-species variability, we recovered a number of target genes of DAF-16, a central regulator of the insulin/IGF pathway in nematodes (Murphy et al., 2003). Knocking down *daf-16* in embryos changed the gene expression profile of *C. elegans* toward the profile of *C. briggsae*. Thus, some of the evolutionary expression changes between both species seem to be a direct consequence of different DAF-16 levels in the embryo. Although the functional consequence of this difference remains to be explored, an adaptive evolution of the insulin/IGF pathway is conceivable because this pathway regulates stress resistance (Tatar et al., 2003; Baumeister et al., 2006) and is therefore likely affected by the environment and life conditions specific to each species.

In conclusion, our findings underscore the relevance of a combined analysis of transcript and protein levels when studying gene regulation during animal development. We provide all of our expression data as a valuable resource to the research community and implemented a publicly available database with graphical representations of all developmental transcript and protein expression profiles at http://elegans.mdc-berlin.de.

EXPERIMENTAL PROCEDURES

Worm Culture and Stable Isotope Labeling and Sample Preparation

C. elegans wild-type strain N2 and *C. briggsae* wild-type strain AF16 were used in this study, cultured as described previously (Brenner, 1974). *C. elegans* and *C. briggsae* were metabolically labeled by feeding either light (Lys0; $^{12}C_6,^{14}N_2$) or heavy (Lys8; $^{13}C_6,^{15}N_2$) SILAC-labeled *E. coli* (Hanke et al., 2008) for at least two generations. Light-labeled staged animals were collected at different time points. An asynchronous reference sample (containing all stages) was produced using heavy-labeled bacteria. Detailed information can be found in the Supplemental Information.

Mass-Spectrometry-Based Protein Quantification

Light and heavy mixtures of SILAC protein extracts (150 μg per sample) were fractioned by SDS-PAGE, in-gel digested using Lysyl endopeptidase (LysC) and cleaned by STAGE tip purification (Rappsilber et al., 2003). Online liquid chromatography-tandem mass spectrometry (LC-MS/MS) analysis was performed essentially as previously described (Selbach et al., 2008), using 10%–60% acetonitril gradients (240 or 360 min) and an LTQ-Orbitrap hybrid mass spectrometer (Thermo Fisher Scientific). The MaxQuant software package and an in-house curated database for *C. elegans*, *C. briggsae* (see the Experimental Procedures), and *E. coli* (MG1655) plus common contaminants (e.g., trypsin, BSA) (v.1.0.13.13) was used to identify and quantify proteins (Cox and Mann, 2008; Cox et al., 2009). False discovery rate was set to 5% (FDR of 5) at both the peptide and protein level (further details are found in the Supplemental Information).

Proteomic Data Validation by Western Blotting

Total protein (20 μg) was separated by SDS-PAGE, blotted onto polyvinylidene fluoride membrane, and analyzed by immunodetection (primary antibodies and GFP strains are listed in the Supplemental Experimental Procedures) using chemiluminescence (PerkinElmer). Films were scanned and quantitative analysis was performed using ImageJ software. TBA-2 or HSP-60 was used for normalization (as indicated).

RNA Isolation and RNA-Seq Library Constructions

Total RNA isolation was performed with TRIzol Reagent (Invitrogen) by following the manufacturer's instructions. PolyA mRNA was purified from 10 μg of total RNA using the Dynabeads mRNA Purification Kit for mRNA Purification from Total RNA (Invitrogen). Details of the library preparation are outlined in the Supplemental Experimental Procedures. Cluster generation and sequencing was performed on the Illumina cluster station and Genome Analyzer IIx according to the manufacturer's instructions. Read lengths were 76 bases.

All details concerning sample collection, data generation, processing, analysis, and validation can be found in the Supplemental Information.

ACCESSION NUMBERS

Data analyzed herein have been deposited in the NCBI Gene Expression Omnibus under accession number GSE53359.

SUPPLEMENTAL INFORMATION

Supplemental Information includes Supplemental Experimental Procedures, six figures, and five tables and can be found with this article online at http://dx.doi.org/10.1016/j.celrep.2014.01.001.

AUTHOR CONTRIBUTIONS

ACKNOWLEDGMENTS

REFERENCES

Baumeister, R., Schaffitzel, E., and Hertweck, M. (2006). Endocrine signaling in Caenorhabditis elegans controls stress response and longevity. J. Endocrinol. *190*, 191–202.

Brenner, S. (1974). The genetics of Caenorhabditis elegans. Genetics *77*, 71–94.

Carroll, S.B. (2008). Evo-devo and an expanding evolutionary synthesis: a genetic theory of morphological evolution. Cell *134*, 25–36.

Cox, J., and Mann, M. (2008). MaxQuant enables high peptide identification rates, individualized p.p.b.-range mass accuracies and proteome-wide protein quantification. Nat. Biotechnol. *26*, 1367–1372.

Cox, J., Matic, I., Hilger, M., Nagaraj, N., Selbach, M., Olsen, J.V., and Mann, M. (2009). A practical guide to the MaxQuant computational platform for SILAC-based quantitative proteomics. Nat. Protoc. *4*, 698–705.

Cutter, A.D. (2008). Divergence times in Caenorhabditis and Drosophila inferred from direct estimates of the neutral mutation rate. Mol. Biol. Evol. *25*, 778–786.

de Sousa Abreu, R., Penalva, L.O., Marcotte, E.M., and Vogel, C. (2009). Global signatures of protein and mRNA expression levels. Mol. Biosyst. *5*, 1512–1526.

Domazet-Lošo, T., and Tautz, D. (2010). A phylogenetically based transcriptome age index mirrors ontogenetic divergence patterns. Nature *468*, 815–818.

Dreszer, T.R., Karolchik, D., Zweig, A.S., Hinrichs, A.S., Raney, B.J., Kuhn, R.M., Meyer, L.R., Wong, M., Sloan, C.A., Rosenbloom, K.R., et al. (2012). The UCSC Genome Browser database: extensions and updates 2011. Nucleic Acids Res. *40* (Database issue), D918–D923.

Frand, A.R., Russel, S., and Ruvkun, G. (2005). Functional genomic analysis of C. elegans molting. PLoS Biol. *3*, e312.

Fredens, J., Engholm-Keller, K., Giessing, A., Pultz, D., Larsen, M.R., Højrup, P., Møller-Jensen, J., and Færgeman, N.J. (2011). Quantitative proteomics by amino acid labeling in C. elegans. Nat. Methods *8*, 845–847.

Geillinger, K.E., Kuhlmann, K., Eisenacher, M., Meyer, H.E., Daniel, H., and Spanier, B. (2012). Dynamic changes of the Caenorhabditis elegans proteome during ontogenesis assessed by quantitative analysis with 15N metabolic labeling. J. Proteome Res. *11*, 4594–4604.

Gerstein, M.B., Lu, Z.J., Van Nostrand, E.L., Cheng, C., Arshinoff, B.I., Liu, T., Yip, K.Y., Robilotto, R., Rechtsteiner, A., Ikegami, K., et al.; modENCODE Consortium (2010). Integrative analysis of the Caenorhabditis elegans genome by the modENCODE project. Science *330*, 1775–1787.

Haerty, W., Artieri, C., Khezri, N., Singh, R.S., and Gupta, B.P. (2008). Comparative analysis of function and interaction of transcription factors in nematodes: extensive conservation of orthology coupled to rapid sequence evolution. BMC Genomics *9*, 399.

Hanke, S., Besir, H., Oesterhelt, D., and Mann, M. (2008). Absolute SILAC for accurate quantitation of proteins in complex mixtures down to the attomole level. J. Proteome Res. *7*, 1118–1130.

Heck, A.J.R., and Krijgsveld, J. (2004). Mass spectrometry-based quantitative proteomics. Expert Rev. Proteomics *1*, 317–326.

Huang, D.W., Sherman, B.T., Zheng, X., Yang, J., Imamichi, T., Stephens, R., and Lempicki, R.A. (2009). Extracting biological meaning from large gene lists with DAVID. Curr. Protoc. Bioinformatics *13*, 13.11.

Johnstone, I.L., and Barry, J.D. (1996). Temporal reiteration of a precise gene expression pattern during nematode development. EMBO J. *15*, 3633–3639.

Kalinka, A.T., Varga, K.M., Gerrard, D.T., Preibisch, S., Corcoran, D.L., Jarrells, J., Ohler, U., Bergman, C.M., and Tomancak, P. (2010). Gene expression divergence recapitulates the developmental hourglass model. Nature *468*, 811–814.

Kim, Dh., Grün, D., and van Oudenaarden, A. (2013). Dampening of expression oscillations by synchronous regulation of a microRNA and its target. Nat. Genet. *45*, 1337–1344.

Krüger, M., Moser, M., Ussar, S., Thievessen, I., Luber, C.A., Forner, F., Schmidt, S., Zanivan, S., Fässler, R., and Mann, M. (2008). SILAC mouse for quantitative proteomics uncovers kindlin-3 as an essential factor for red blood cell function. Cell *134*, 353–364.

Larance, M., Bailly, A.P., Pourkarimi, E., Hay, R.T., Buchanan, G., Coulthurst, S., Xirodimas, D.P., Gartner, A., and Lamond, A.I. (2011). Stable-isotope labeling with amino acids in nematodes. Nat. Methods *8*, 849–851.

Levin, M., Hashimshony, T., Wagner, F., and Yanai, I. (2012). Developmental milestones punctuate gene expression in the Caenorhabditis embryo. Dev. Cell *22*, 1101–1108.

Looso, M., Borchardt, T., Krüger, M., and Braun, T. (2010). Advanced identification of proteins in uncharacterized proteomes by pulsed in vivo stable isotope labeling-based mass spectrometry. Mol. Cell. Proteomics *9*, 1157–1166.

Mangone, M., Manoharan, A.P., Thierry-Mieg, D., Thierry-Mieg, J., Han, T., Mackowiak, S.D., Mis, E., Zegar, C., Gutwein, M.R., Khivansara, V., et al. (2010). The landscape of C. elegans 3'UTRs. Science *329*, 432–435.

Moss, E.G. (2007). Heterochronic genes and the nature of developmental time. Curr. Biol. *17*, R425–R434.

Murphy, C.T., McCarroll, S.A., Bargmann, C.I., Fraser, A., Kamath, R.S., Ahringer, J., Li, H., and Kenyon, C. (2003). Genes that act downstream of DAF-16 to influence the lifespan of Caenorhabditis elegans. Nature *424*, 277–283.

Ong, S.-E., Blagoev, B., Kratchmarova, I., Kristensen, D.B., Steen, H., Pandey, A., and Mann, M. (2002). Stable isotope labeling by amino acids in cell culture, SILAC, as a simple and accurate approach to expression proteomics. Mol. Cell. Proteomics *1*, 376–386.

Page, A.P., and Johnstone, I.L. (2007). The cuticle. WormBook *19*, 1–15.

Peter, I.S., and Davidson, E.H. (2011). Evolution of gene regulatory networks controlling body plan development. Cell *144*, 970–985.

Rappsilber, J., Ishihama, Y., and Mann, M. (2003). Stop and go extraction tips for matrix-assisted laser desorption/ionization, nanoelectrospray, and LC/MS sample pretreatment in proteomics. Anal. Chem. *75*, 663–670.

Ruvkun, G., and Giusto, J. (1989). The Caenorhabditis elegans heterochronic gene lin-14 encodes a nuclear protein that forms a temporal developmental switch. Nature *338*, 313–319.

Schrimpf, S.P., Weiss, M., Reiter, L., Ahrens, C.H., Jovanovic, M., Malmström, J., Brunner, E., Mohanty, S., Lercher, M.J., Hunziker, P.E., et al. (2009). Comparative functional analysis of the Caenorhabditis elegans and Drosophila melanogaster proteomes. PLoS Biol. *7*, e48.

Schwanhäusser, B., Busse, D., Li, N., Dittmar, G., Schuchhardt, J., Wolf, J., Chen, W., and Selbach, M. (2011). Global quantification of mammalian gene expression control. Nature *473*, 337–342.

Selbach, M., Schwanhäusser, B., Thierfelder, N., Fang, Z., Khanin, R., and Rajewsky, N. (2008). Widespread changes in protein synthesis induced by microRNAs. Nature *455*, 58–63.

St Johnston, D., and Nüsslein-Volhard, C. (1992). The origin of pattern and polarity in the Drosophila embryo. Cell *68*, 201–219.

Stadler, M., and Fire, A. (2013). Conserved translatome remodeling in nematode species executing a shared developmental transition. PLoS Genet. *9*, e1003739.

Stein, L.D., Bao, Z., Blasiar, D., Blumenthal, T., Brent, M.R., Chen, N., Chinwalla, A., Clarke, L., Clee, C., Coghlan, A., et al. (2003). The genome sequence of Caenorhabditis briggsae: a platform for comparative genomics. PLoS Biol. *1*, E45.

Sulston, J.E., Schierenberg, E., White, J.G., and Thomson, J.N. (1983). The embryonic cell lineage of the nematode Caenorhabditis elegans. Dev. Biol. *100*, 64–119.

Sury, M.D., Chen, J.-X., and Selbach, M. (2010). The SILAC fly allows for accurate protein quantification in vivo. Mol. Cell. Proteomics *9*, 2173–2183.

Tabuse, Y., Nabetani, T., and Tsugita, A. (2005). Proteomic analysis of protein expression profiles during Caenorhabditis elegans development using two-dimensional difference gel electrophoresis. Proteomics *5*, 2876–2891.

Tatar, M., Bartke, A., and Antebi, A. (2003). The endocrine regulation of aging by insulin-like signals. Science *299*, 1346–1351.

Uyar, B., Chu, J.S.C., Vergara, I.A., Chua, S.Y., Jones, M.R., Wong, T., Baillie, D.L., and Chen, N. (2012). RNA-seq analysis of the C. briggsae transcriptome. Genome Res. *22*, 1567–1580.

Weiss, M., Schrimpf, S., Hengartner, M.O., Lercher, M.J., and von Mering, C. (2010). Shotgun proteomics data from multiple organisms reveals remarkable quantitative conservation of the eukaryotic core proteome. Proteomics *10*, 1297–1306.

Zhao, Z., Boyle, T.J., Bao, Z., Murray, J.I., Mericle, B., and Waterston, R.H. (2008). Comparative analysis of embryonic cell lineage between Caenorhabditis briggsae and Caenorhabditis elegans. Dev. Biol. *314*, 93–99.